

## BIOLOGY CONTRIBUTION

# EFFECTS OF FRACTIONATED RADIATION ON THE BRAIN VASCULATURE IN A MURINE MODEL: BLOOD–BRAIN BARRIER PERMEABILITY, ASTROCYTE PROLIFERATION, AND ULTRASTRUCTURAL CHANGES

HONG YUAN, PH.D.,\*<sup>†</sup> M. WALEED GABER, PH.D.,\* KELLI BOYD, D.V.M., PH.D.,<sup>‡</sup>  
CHRISTY M. WILSON, M.S.,\* MOHAMMAD F. KIANI, PH.D.,<sup>§</sup> AND  
THOMAS E. MERCHANT, D.O., PH.D.<sup>†\*</sup>

\*Department of BioImaging, College of Health Science Engineering, University of Tennessee Health Science Center, Memphis, TN; <sup>†</sup>Department of Radiological Sciences, St. Jude Children's Research Hospital, Memphis, TN; <sup>‡</sup>Animal Research Center, St. Jude Children's Research Hospital, Memphis, TN; and <sup>§</sup>Departments of Mechanical Engineering and Radiation Oncology, Temple University, Philadelphia, PA

**Purpose:** Radiation therapy of CNS tumors damages the blood–brain barrier (BBB) and normal brain tissue. Our aims were to characterize the short- and long-term effects of fractionated radiotherapy (FRT) on cerebral microvasculature in mice and to investigate the mechanism of change in BBB permeability in mice.

**Methods and Materials:** Intravital microscopy and a cranial window technique were used to measure BBB permeability to fluorescein isothiocyanate (FITC)-dextran and leukocyte endothelial interactions before and after cranial irradiation. Daily doses of 2 Gy were delivered 5 days/week (total, 40 Gy). We immunostained the molecules to detect the expression of glial fibrillary acidic protein and to demonstrate astrocyte activity in brain parenchyma. To relate the permeability changes to endothelial ultrastructural changes, we used electron microscopy.

**Results:** Blood-brain barrier permeability did not increase significantly until 90 days after FRT, at which point it increased continuously until 180 days post-FRT. The number of adherent leukocytes did not increase during the study. The number of astrocytes in the cerebral cortex increased significantly; vesicular activity in endothelial cells increased beginning 90 days after irradiation, and most tight junctions stayed intact, although some were shorter and less dense at 120 and 180 days.

**Conclusions:** The cellular and microvasculature response of the brain to FRT is mediated through astrogliosis and ultrastructural changes, accompanied by an increase in BBB permeability. The response to FRT is delayed as compared with single-dose irradiation treatment, and does not involve leukocyte adhesion. However, FRT induces an increase in the BBB permeability, as in the case of single-dose irradiation. © 2006 Elsevier Inc.

Blood–brain barrier, Fractionated radiotherapy, Radiation toxicity, Permeability, Astrogliosis.

## INTRODUCTION

Radiation therapy directed at brain tumors can damage the glial, neuronal, and vasculature compartments of the brain, limiting the doses of radiation that can be safely delivered to patients (1–4). The causes and interconnections of the side effects of radiation treatment are not yet fully understood (5). Our studies, as well as those of others, have shown that ionizing radiation can disrupt the blood–brain barrier (BBB) This disruption may exacerbate radiation-induced brain toxicity (5–9). Research into irradiation effects in

normal brain tissue has been principally limited to studies of single-dose irradiation (5, 6, 9–12). However, large single doses of radiation are not commonly used in the clinic; exceptions include radiosurgery, pulsed high-dose-rate brachytherapy, and some hypofractionated palliative treatment regimens. Although fractionated radiotherapy (FRT) is the leading mode of radiation delivery, the effects of fractionated doses of ionizing radiation on the brain microvasculature have not been thoroughly investigated (13–15). In previous studies (16), we have observed a difference in cellular response to fractionated and single-dose brain treat-

Reprint requests to: M. Waleed Gaber, Ph.D., Department of BioImaging, College of Health Science Engineering, University of Tennessee Health Science Center Memphis, TN 38163. Tel: (901) 448-3170; Fax: (901) 448-7387; E-mail: wgaber@utmem.edu

Supported in part by beginning Grant-in-Aid no. AHA 0365250B from the southeast affiliate of the American Heart Association, Alma and Hal Reagan Fellowship (C.M. Wilson), Cancer Center Support Grant CA 21765 from The National Cancer

Institute, and by the American Lebanese Syrian Associated Charities.

**Acknowledgments**—The authors thank John F. Killmar for technical assistance with the animal surgery and Ms. Margaret Carbaugh, Senior Scientific Editor, St. Jude Children's Research Hospital, for editorial assistance with the manuscript.

Received Feb 6, 2006, and in revised form June 19, 2006.  
Accepted for publication June 20, 2006.

ments; the single-dose–response was rapid, within hours of treatment, whereas the fractionated response was delayed until the end of treatment (30 days) (16).

In a previous study (9), we characterized the effects of large single doses of irradiation on the cerebral microvasculature, showing that ionizing radiation increases the BBB permeability to fluorescein isothiocyanate (FITC)-dextran molecules of various sizes. We also found that the increased BBB permeability is associated with an increase in cell adhesion (9), findings that are consistent with those of other researchers (13, 14, 17, 18).

In the current study, we characterized the acute effects (during and right after), as well as the long-term effects (up to 180 days postirradiation) of fractionated irradiation on BBB permeability in normal mouse brain pial vessels. Intravital microscopy and a closed cranial window technique were used. Using immunohistochemistry and electron microscopy (EM) techniques, we also investigated the relationship between changes in the ultrastructure of the brain and the irradiation-induced changes in BBB permeability. This study develops a fractionated RT animal model that was used to study the radiation-induced changes in BBB permeability, endothelial cell adhesion, structural changes caused by radiation, as well as the cellular response, especially astrocytic activity. The model can be used further to study interventional methods aimed at ameliorating the side effects of RT.

## METHODS AND MATERIALS

### *Animals*

Male C57BL/6J mice (6–7 weeks of age) were purchased from Harlan Laboratories (Frederick, MD) and used in the study. All protocols followed were approved by the Animal Care and Use Committees of St. Jude Children's Research Hospital and the University of Tennessee Health Science Center (Memphis, TN). We also followed the policy guidelines of the National Institutes of Health for the humane care and use of laboratory animals.

### *Cranial window preparation*

Cranial window surgery was performed according to our previously published protocol (19). Briefly, animals were anesthetized with an i.m. injection of a solution of ketamine (100 mg/kg) and xylazine (10 mg/kg). The animals were then placed in a stereotaxic frame (Kopf Instruments, Tujunga, CA). We removed the scalp, underlying soft tissue, skull bone, and dura. A 4 × 6 mm glass window that extended from the bregma to lambdoid sutures and was centered on the midsagittal suture was placed and fixed over the surgically exposed cerebral cortex using cyanoacrylate glue. After surgery, animals were allowed to recover for 1 week before data collection was initiated.

### *Experimental design*

Mice were divided into two study groups. In the acute effects group ( $n = 6$ ), cranial window surgery was conducted 1 week before the start of the fractionated irradiation, and BBB permeability was measured after 1, 2, 5, 10, 15, and 20 irradiation fractions (1 radiation fraction per day). Each animal served as its own control. Animals in the long-term effect group ( $n = 40$ ) were

subdivided into 4 groups (each with 10 animals) on the basis of time from the start of the fractionated radiation: 60 days, 90 days, 120 days, and 180 days. Each long-term effect group included irradiated mice ( $n = 6$ ) and sham mice ( $n = 4$ ); cranial window surgery was conducted on all animals in the long-term group 1 week before the measurements started. BBB permeability and cell adhesion were measured in all of the animals in the long-term groups at 60, 90, 120, and 180 days from the start of fractionated irradiation.

This schedule was designed to allow us to follow the acute and long-term effects of brain irradiation. As there was no precedence to go by, we chose 1 month as an adequate interval to follow the changes induced by FRT. Experiments were terminated at 180 days after the start of FRT (equivalent to one quarter of the life expectancy of the mice), which we considered to be sufficient to observe the long-term changes induced by radiation treatment.

### *Radiation treatment*

All radiation treatments were administered with a 6-MV X-ray linear accelerator (Siemens Primus, Concord, CA). Fractionated irradiation was delivered to the whole brains of the mice at a daily dose of 2 Gy, 5 days/week for 4 weeks, for a total of 40 Gy. Animals were placed in a customized chamber, which could hold 12 mice, connected to a gas anesthesia (2% isoflurane) machine. Animals were placed on a fluoroscopy unit (Phillips Medical Systems, New York, NY) radiation simulator (Siemens, Concord, CA) to determine the treatment area, and a customized lead shielding block (17 cm × 17 cm) was molded according to the measured area. During irradiation, the customized, lead shielding block covered the bodies of the animals to ensure that only the brains were irradiated. Tissue-equivalent material (1 cm thick) was placed above the head of each animal to establish electronic equilibrium. To ensure proper positioning of the animals, they were imaged during irradiation using the digital portal system EPID (Siemens, Concord, CA).

### *BBB permeability and cell adhesion measurement*

Measurement of BBB permeability and cell adhesion using intravital microscopy has previously been detailed (9, 19). Briefly, to visualize cerebral microcirculation, animals were anesthetized with a solution of ketamine and xylazine, as described above, and placed in a stereotaxic frame under a fluorescence intravital microscope. As a permeability tracer, we used FITC-dextran molecules (Sigma, St. Louis, MO) with molecular sizes of 4.4 and 38.2 kD. Before dye injection, a microvascular region with 2 to 3 venules and clear parenchymal tissue was chosen, and a reference image (for localization of vessel) was first recorded under epifluorescence illumination. A bolus of FITC-dextran in saline (10 mg/kg body weight) was injected through the retro-orbital vein. To minimize fluorophore excitation, changes in brain tissue intensity levels were digitally recorded after injection every 1 s for the first 60 s, every 30 s for 5 min, and then every 1 min for 20 min. The images were later analyzed off-line by using MetaMorph software (Universal Imaging Co., West Chester, PA) to measure the extravasation rate of FITC-dextran from vessels to tissue, which is proportional to the slope of the change of tissue intensity vs. time (19).

Leukocyte adhesion was measured by injecting Rhodamine-6G (0.4 mg/kg body weight; Sigma, St. Louis, MO) through the retro-orbital vein to stain the leukocytes. A leukocyte in contact with the vessel wall was considered to be adherent if it did not move for 30 s; this measure is expressed as the number of adherent

cells per 100- $\mu\text{m}$  length of vessel (19). The measurements were conducted in venules with diameters ranging from 30 to 45  $\mu\text{m}$ . Permeability and adhesion measurements were carried out in the same vessels for each animal at each time point, before and after irradiation.

#### Immunohistochemistry and electron microscopy

To investigate the cellular response in the irradiated brain's parenchyma, we quantified the activity of astrocytes using immunostaining methods. Measurements were conducted at the end of treatment (30 days) and at 60, 90, 120, and 180 days after the start of irradiation. Using the same time points, we used EM to examine changes in the ultrastructure of the cerebral vasculature.

We perfused heparinized saline (0.9%) for 60 s through the left ventricle of the hearts of the anesthetized mice, after which we infused paraformaldehyde and glutaraldehyde (4% and 2%, respectively) mixed in 0.05 M phosphate buffer (pH 7.4). Whole brain tissue was removed and cut into right and left hemispheres. The left hemisphere was used for immunostaining, and the right hemisphere for EM studies (described later here). The hemisphere of the brain to be immunostained was then embedded in paraffin and cut into 4- $\mu\text{m}$  coronal sections.

Rabbit antihuman glial fibrillary acidic protein (GFAP; catalog no. Z0334), and rabbit immunoglobulins (negative control; catalog no. X0903) were purchased from DAKO (Carpinteria, CA). The secondary antibody for GFAP, biotinylated goat antirabbit, was purchased from Vector (catalog no. BA-1000; Burlingame, CA) and used at a 1:200 dilution. Immunohistochemistry assays were performed on the DAKO autostainer at room temperature. Light microscopic images were captured using a digital imaging system (Spot Insight Color, Diagnostic Instruments) and the image analysis was performed using Image Pro Plus software (Version, 4.5.0.19; Media Cybernetics, Inc., Silver Spring, MD).

The number of GFAP-stained astrocytes was counted in five fields at  $\times 400$  magnification in the cerebral cortex overlying the dentate gyrus of the hippocampus, and in the hippocampus itself. These areas were chosen because they are identifiable, which ensures that counts are performed in similar locations in all brains. The brains of irradiated animals were compared with those of sham-irradiated controls at the time points listed above.

After transcardiac perfusion (described above), a small block of mouse brain cortex (approximately 1-mm cube) was cut from the right hemisphere above the corpus callosum area. The block was further fixed in 2% phosphate-buffered saline (PBS)-glutaraldehyde and then in 1% Osmium. The tissue block was stepwise dehydrated in ethanol and block-stained with saturated uranyl acetate, embedded in Araldite, and sectioned using an Ultracut FCR ultramicrotome. Semithin sections (0.6  $\mu\text{m}$ ) were stained with Toluidine Blue dye; ultrathin sections (50 nm) were stained with lead citrate, mounted on Pioloform-coated copper grids, and examined by using a JEOL transmission electron microscope (JEOL TEM 1200EXII). All chemicals were purchased from Electron Microscopy Sciences (Hatfield, PA).

#### Statistical analysis

Statistical analyses were conducted using SigmaStat software (version 2.03, SPSS Science, Chicago, IL). The short-term effects of fractionated irradiation on permeability were determined by repeated-measures analysis of variance (ANOVA), and a multiple comparison procedure (Dunnett test) was used to discriminate

Table 1. Animal weight throughout the course of experiment

Day	Sham*	FRT*	<i>p</i> -value
0	19.00 $\pm$ 0.58	19.75 $\pm$ 0.23	0.28
14	21.34 $\pm$ 0.88	21.00 $\pm$ 0.25	0.67
30	24.43 $\pm$ 0.39	21.90 $\pm$ 0.23	0.001
60	27.39 $\pm$ 0.84	25.57 $\pm$ 0.52	0.05
90	30.27 $\pm$ 1.01	27.05 $\pm$ 0.57	0.01
120	30.65 $\pm$ 0.64	27.03 $\pm$ 1.40	0.05
180	33.53 $\pm$ 0.59	29.14 $\pm$ 0.53	0.001

Abbreviation: FRT = fractionated radiotherapy.

\* Data presented as average weight (g)  $\pm$  SEM. Minimum of 3 animals in sham group and 10 animals in FRT group.

among the means. Results of long-term effects of fractionated irradiation on BBB permeability and cell adhesion were compared with sham animal data using Student's *t* test. Data are presented as mean  $\pm$  SEM, and differences between the means were considered to be statistically significant at a probability of  $p < 0.05$ .

## RESULTS

#### Acute effects of FRT on BBB permeability

Changes in BBB permeability to 4.4-kD FITC-dextran were measured before irradiation and after the Fractions 1, 2, 3, 5, 10, 15, and 20. Before irradiation, BBB permeability to 4.4 kD FITC-dextran was  $13.7 \pm 1.6 \times 10^{-7}$  cm/s. During the FRT period, we observed no significant change in permeability ( $p = 0.615$ ); values ranged from  $13.2 \times 10^{-7}$  to  $19.2 \times 10^{-7}$  cm/s (data not shown).

#### Long-term effects of FRT on BBB permeability

Mice treated with fractionated irradiation were kept in the animal facility up to 180 days from the start of FRT. On the basis of gross observations, irradiated mice experienced no specific deficits such as ataxia, paresis, or seizures; our observations of the sham-treated mice were similar. However, the hair of the irradiated mice turned gray and white, especially between the neck and the head, beginning 90 days from the start of FRT. The irradiated animals' average weight was significantly less than that of the sham-treated animals beginning 30 days from the start of FRT (Table 1). Two of the 24 irradiated animals died of unknown causes (one at 95 days, the other at 120 days after the start of FRT). No animals from the sham-treated group died during the course of these experiments.

In the long-term effects group, we used two different molecular sizes of FITC-dextran (4.4 and 38.2 kD) for BBB permeability measurements. Our results indicate that in irradiated mice, the permeability to both tracers significantly increased ( $p < 0.05$ ). Results are shown in Fig. 1.

#### Leukocyte adhesion in pial venules

To investigate the possibility of a relationship between the observed permeability increase and leukocyte-endothelial cell interactions similar to what we observed in the single-dose irradiation study (9), we used intravital micros-

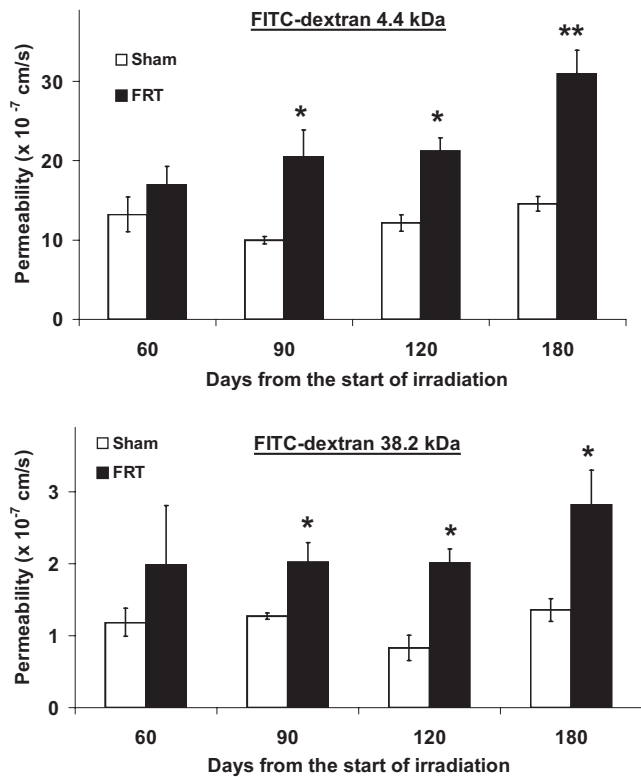


Fig. 1. Long-term changes in blood–brain barrier (BBB) permeability to both FITC-dextran 4.4 kD (top) and 38.2 kD (bottom) molecules. A significant difference was observed 90 days from the start of irradiation and persisted throughout the experiment (180 days) (\* $p < 0.05$ , \*\* $p < 0.01$ ).

copy to record leukocyte activity in the pial venules of both irradiated and sham mice. No significant difference was observed in the number of adherent leukocytes or in vessel diameter of irradiated and sham animals (data not shown).

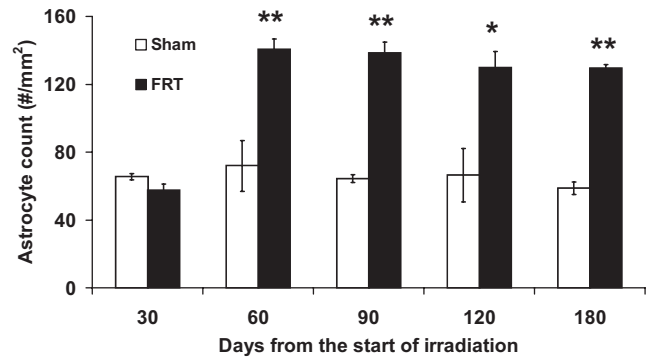


Fig. 3. Number of glial fibrillary acidic protein (GFAP)–positive astrocytes in the cerebral cortex of irradiated and sham mice. At 60 days, the number of positive cells in irradiated mice was double that of sham animals, a difference that persisted throughout the experiments (\* $p < 0.05$ , \*\* $p < 0.01$ ).

#### Immunohistochemistry study

We compared the average number of GFAP-stained astrocytes of sham-treated and irradiated animals from 5 fields at  $\times 400$  magnification. Figure 2 shows a typical GFAP staining in a mouse cerebral cortex over the hippocampus. By 60 days from the start of FRT, the number of GFAP-positive cells in the cerebral cortex of irradiated mice was double that of the sham mice ( $141 \pm 6 / \text{mm}^2$  vs.  $72 \pm 15 / \text{mm}^2$ ), and the number of cells remained significantly higher throughout the experiment (Fig. 3). However, in the hippocampus, the number of astrocytes in the sham-treated and irradiated groups did not differ significantly at any of the time points (data not shown).

#### Ultrastructural changes in cerebral endothelial cells

The microscopic images from sham-treated animals showed normal endothelial structures with well-pre-

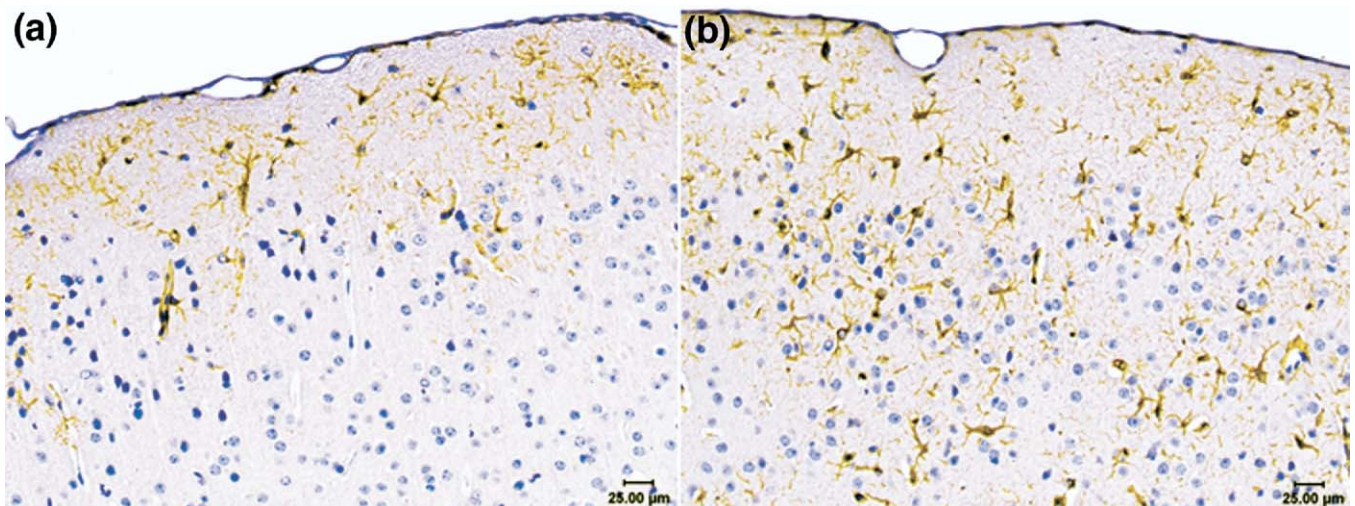


Fig. 2. Glial fibrillary acidic protein (GFAP)–immunostained astrocytes from the brain of an irradiated mouse (a) and sham mouse (b). Astrocytes and their processes stain dark brown. Irradiation caused an increase in astrocyte processes and cell numbers in the cerebral cortex. Both sections are from the cerebral cortex overlying the dentate gyrus of the hippocampus.

## DISCUSSION

Our aim was to characterize the short- and long-term effects of fractionated radiation therapy on the cerebral microvasculature of the brain in mice. Determination of these effects is important because research of irradiation effects in normal brain tissue has been largely limited to studies of single-dose irradiation, although fractionated radiation is more commonly used in the clinic. Our observations led us to conclude that BBB permeability did not increase until 90 days postirradiation and that astrocyte proliferation increased significantly, beginning 60 days postirradiation.

Vesicular activity in the cytoplasm increased notably starting 90 days from the start of FRT, and 30 days from the start of FRT the average weight of irradiated animals was significantly lower than that of the sham-treated animals. However, leukocyte adhesion did not increase significantly during the course of the experiments, and we observed no significant increase in BBB permeability during the fractionated irradiation treatment period, which indicates a slow and delayed response to FRT. In contrast, we have previously observed a significant increase in permeability as early as 24 h after a single fraction of 20 Gy irradiation (9). This difference in response agrees with the results that we previously reported (16) regarding the differences in TNF- $\alpha$  and ICAM-1 expression resulting from large single-fraction and fractionated irradiation of the mouse brain. These findings led Gaber *et al.* (16) to conclude that the molecular response to single-dose irradiation is rapid, whereas the response to fractionated irradiation is slow.

Leukocyte rolling and adhesion after single-dose radiation treatments have been reported (20), and they are thought to be involved in irradiation-induced vascular injury. We have previously shown that, in the case of single-dose irradiation treatment, the observed increase in permeability has been accompanied by an increase in leukocyte adhesion through the ICAM-1 pathway (9). Also, when using antibody-conjugated fluorescent microspheres, Yuan *et al.* (21) observed an upregulation of ICAM-1, E-, and P-selectin to functional levels after treatment with a single dose of 20 Gy irradiation. In the present study we did not observe a significant change in leukocyte adhesion at any time point examined.

Radiation has been reported to cause an inflammatory response in the parenchyma of the mouse brain through the activation of astrocytes and microglial cells (22–24). Ciccirello *et al.* (25) reported activated astrocytes 90 days after treatment with the same dose of fractionated irradiation used in our study. Mildenerger *et al.* (26) also observed a microglial response 6 months after fractionated irradiation. Furthermore, Reuss *et al.* and Willis *et al.* (27, 28) have reported that an inhibition of astrocyte proliferation can affect the BBB integrity. In our experiments (see Fig. 3), we observed an activated astrocyte response 60 days from the start of irradiation that persisted throughout the experiment, a result consistent with previous reports. No significant

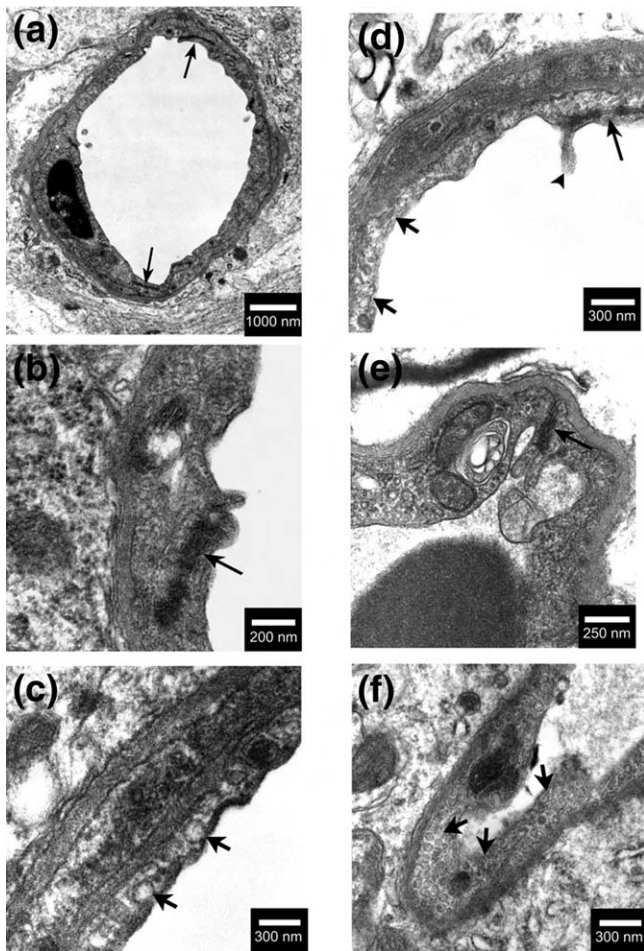


Fig. 4. Representative images from our electron microscopy studies. (a) Normal cerebral microvessel and endothelial cells. Intact tight junctions (long black arrows) are present between adjacent endothelial cells. Note the lack of vesicles in the endothelial cell cytoplasm. (b, c) Cerebral endothelial cells from irradiated mice at 90 days from the start of fractionated radiotherapy (FRT). The intact tight junction is marked by a long black arrow in (b). Many vesicles (thick black arrows) are observed in the cytoplasm in (c). (d) Cerebral endothelial cells from irradiated mice at 120 days from the start of FRT. Tight junctions are shortened (long black arrow) and some membranes are disrupted (black arrowhead). Many vesicles can be seen (thick black arrows). (e, f) Cerebral endothelial cells from irradiated mice at 180 days from the start of FRT. Tight junctions are shortened in irradiated animals (long black arrow) in (e), and many vesicles can be seen in cytoplasm (thick black arrow) in (f).

served tight junctions, very few vesicles, and well-connected basal lamina (Fig. 4a). In irradiated animals, we found that most tight junctions were intact at 90, 120, and 180 days from the start of FRT, although some were shortened and less dense at 120 and 180 days (Fig. 4b–f). However, we observed significantly increased vesicular activities in cerebral endothelial cells at 90, 120, and 180 days from the start of FRT (Fig. 4b–f). We also observed leaflets of external endothelial cell membrane separated from the surface at 120 days (Fig. 4d).

change was observed at 30 days (end of fractionated period), a result that agrees with our findings showing no change in permeability at the same time point. Although radiation-induced gliosis is not directly indicative of inflammation, it is associated with or is a byproduct of brain inflammation. Hwang *et al.*, (29) concluded that irradiated microglia induce the activation of astrocytes through their release of PGE<sub>2</sub>, a metabolic product of the cyclooxygenase-2 (COX-2) enzyme, which is also involved in brain injury. Magnus *et al.* (30) suggest that astrocytes might act as phagocytes to supplement microglial phagocytic activity in the inflamed CNS.

Electron microscopic images revealed an increase in vesicular activity concomitant with our observed permeability changes (Fig. 4). Vesicles in endothelial cells are one of the transport pathways across the BBB, and increased vesicular activities were observed in several studies of the inflammatory response in different diseases (31, 32). D'Avella *et al.* (13, 33) observed increased BBB permeability and an increase in the number of vesicles 15 and 90 days after the same dose of fractionated irradiation. They used the quantitative <sup>14</sup>C-aminoisobutyric acid (AIB) technique coupled with an EM study. Their finding agrees with our observations; however, the difference in the onset of change between our results and theirs may be explained by their use of different permeability tracers. The AIB compound (13), a small molecule with an 0.9-angstrom radius and a molecular weight of 103 D, is much smaller than the molecules used in our studies and hence might be more permeable through the BBB. However, the presence of tumors makes it necessary to be cautious when comparing their findings with ours. In agreement with our findings, D'Avella (13, 33) reported no damage to the tight junctions 90 days after fractionated irradiation. Debbage *et al.* (14) also reported an increase in permeability and vesicular activity after 42 Gy fractionated

irradiation to murine adenocarcinomas in mice. It is important to note that although our permeability measurements were conducted in the pial layer the observed astrogliosis, increased vesicular activity and tight junction changes were observed in the parenchyma of the cerebral cortex. The difference between pial and parenchymal microvessels has been previously established (34). However, Revest *et al.* (35) showed that, similar to the parenchymal vessels, the pial vessels exhibit high transendothelial electrical resistance and tight junctions, confirming that they reflect the main structural properties of the BBB. Although this similarity between the pial and parenchymal vessels could indicate that their response to late radiation injury might be equivalent, it does not necessarily imply that their responses are identical and differences between them might exist.

## CONCLUSION

In conclusion, radiation effects on the brain vasculature are of crucial importance in the progression of radiation-induced CNS toxicity. Although our results do not point toward a specific mechanism behind the observed changes, we speculate that an inflammatory cascade has initiated these changes. One possible cause of this conjectured inflammatory cascade could be direct cell death resulting from the irradiation injury. In this work we have characterized part of the vascular changes induced by fractionated doses of irradiation, and our results indicate a delayed response expressed by a significant increase in activated astrocytes and an increase in vesicular activity. We conclude that the cellular and microvascular response to fractionated irradiation is mediated through changes in the ultrastructure of the brain accompanied by an increase in BBB permeability. In future studies we will attempt to elucidate the mechanisms connecting these two observed facets of radiation response in the case of fractionated irradiation.

## REFERENCES

1. Stone HB, McBride WH, Coleman CN. Modifying normal tissue damage postirradiation report of a workshop sponsored by the radiation research program, National Cancer Institute, Bethesda, MD, September 6–8, 2000. *Radiat Res* 2002;157:204–223.
2. Madsen TM, Kristjansen PEG, Bowlwig TG, *et al.* Arrested neuronal proliferation and impaired hippocampal function following fractionated brain irradiation in the adult rat. *Neuroscience* 2003;119:635–642.
3. Wong CS, Van Der Kogel AJ. Mechanisms of radiation injury to the central nervous system: implications for neuroprotection. *Mol Interv* 2004;4:273–284.
4. Tofilon PJ, Fike JR. The radioreponse of the central nervous system: A dynamic process. *Radiat Res* 2000;153:357–370.
5. Belka C, Budach W, Kortmann RD, *et al.* Radiation induced CNS toxicity—molecular and cellular mechanisms. *Br J Cancer* 2001;85:1233–1239.
6. Acker JC, Marks LB, Spencer DP, *et al.* Serial *in vivo* observations of cerebral vasculature after treatment with a large single fraction of radiation. *Radiat Res* 1998;149:350–359.
7. Anscher MS, Chen L, Rabbani Z, *et al.* Recent progress in defining mechanisms and potential targets for prevention of normal tissue injury after radiation therapy. *Int J Radiat Oncol Biol Phys* 2005;62:255–259.
8. Nordal RA, Wong CS. Molecular targets in radiation-induced blood-brain barrier disruption. *Int J Radiat Oncol Biol Phys* 2005;62:279–287.
9. Yuan H, Gaber MW, McColgan T, *et al.* Radiation-induced permeability and leukocyte adhesion in the rat blood-brain barrier: Modulation with anti-ICAM-1 antibodies. *Brain Res* 2003;969:59–69.
10. Wood K, Jawahar A, Smelley C, *et al.* Exposure of brain to high-dose, focused gamma rays irradiation produces increase in leukocytes-adhesion and paving in small intracerebral blood vessels. *Neurosurgery* 2005;57:1282–1288.
11. Nguyen V, Gaber MW, Sontag MR, *et al.* Late effects of ionizing radiation on microvascular networks in normal tissue. *Radiat Res* 2000;154:531–536.
12. Munter MW, Karger CP, Reith W, *et al.* Delayed vascular injury after single high-dose irradiation in the rat brain: Histologic immunohistochemical, and angiographic studies. *Radiology* 1999;212:475–482.
13. D'Avella D, Ciccirello R, Albiero F, *et al.* Quantitative study

- of blood-brain barrier permeability changes after experimental whole-brain radiation. *Neurosurgery* 1992;30:30–34.
14. Debbage PL, Seidl S, Kreczy A, *et al.* Vascular permeability and hyperpermeability in a murine adenocarcinoma after fractionated radiotherapy: An ultrastructural tracer study. *Histochem Cell Biol* 2000;114:259–275.
  15. Brown WR, Thore CR, Moody DM, *et al.* Vascular damage after fractionated whole-brain irradiation in rats. *Radiat Res* 2005;164:662–668.
  16. Gaber MW, Sabek OM, Fukatsu K, *et al.* The differences in ICAM-1 and TNF- $\alpha$  expression between high single fractions and fractionated irradiation in mouse brain. *Int J Radiat Biol* 2003;79:359–366.
  17. Remler MP, Marcussen WH, Tiller-Borsich J. The late effects of radiation on the blood brain barrier. *Int J Radiat Oncol Biol Phys* 1986;12:1965–1969.
  18. Trnovec T, Kallay Z, Bezek S. Effects of ionizing radiation on the blood brain barrier permeability to pharmacologically active substances. *Int J Radiat Oncol Biol Phys* 1990;19:1581–1587.
  19. Gaber MW, Yuan H, Killmar JT, *et al.* An intravital microscopy study of radiation-induced changes in permeability and leukocyte-endothelial cell interactions in the microvessels of the rat pia mater and cremaster muscle. *Brain Res Brain Res Protoc* 2004;13:1–10.
  20. Quarumby S, Kumar P, Kumar S. Radiation-induced normal tissue injury: Role of adhesion molecules in leukocyte-endothelial cell interactions. *Int J Cancer* 1999;82:385–395.
  21. Yuan H, Goetz DJ, Gaber MW, *et al.* Radiation-induced up-regulation of adhesion molecules in Brain microvasculature and their modulation by dexamethasone. *Radiat Res* 2005;163:544–551.
  22. Chiang CS, McBride WH, Withers HR. Radiation-induced astrocytic and microglial responses in mouse brain. *Radiother Oncol* 1993;29:60–68.
  23. Price RE, Langford LA, Jackson EF, *et al.* Radiation-induced morphologic changes in the rhesus monkey (*Macaca mulatta*) brain. *J Med Primatol* 2001;30:81–87.
  24. Monje ML, Palmer T. Radiation injury and neurogenesis. *Curr Opin Neurol* 2003;16:129–134.
  25. Ciccariello R, d'Avella D, Gagliardi ME, *et al.* Time-related ultrastructural changes in an experimental model of whole brain irradiation. *Neurosurgery* 1996;38:772–779.
  26. Mildnerberger M, Beach TG, McGeer EG, *et al.* An animal model of prophylactic cranial irradiation: Histologic effects at acute, early and delayed stages. *Int J Radiat Oncol Biol Phys* 1990;18:1051–1060.
  27. Reuss B, Dono R, Unsicker K. Functions of fibroblast growth factor (FGF)-2 and FGF-5 in astrological differentiation and blood-brain barrier permeability: Evidence from mouse mutants. *J Neurosci* 2003;23:6404–6412.
  28. Willis CL, Leach L, Clarke GJ, *et al.* Reversible disruption of tight junction complexes in the rat blood-brain barrier, following transitory focal astrocyte loss. *Glia* 2004;48:1–13.
  29. Hwang SY, Jung JS, Kim TH, *et al.* Ionizing radiation induces astrocyte gliosis through microglia activation. *Neurobiol Dis* 2006;21:457–467.
  30. Magnus T, Chan A, Linker RA, *et al.* Astrocytes are less efficient in the removal of apoptotic lymphocytes than microglia cells: implications for the role of glial cells in the inflamed central nervous system. *J Neuropathol Exp Neurol* 2002;61:760–766.
  31. Preston E, Foster DO. Evidence for pore-like opening of the blood-brain barrier following forebrain ischemia in rats. *Brain Res* 1997;761:4–10.
  32. Renkin EM. Multiple pathways of capillary permeability. *Circ Res* 1977;41:735–743.
  33. d'Avella D, Ciccariello R, Angileri FF, *et al.* Radiation-induced blood-brain barrier changes: Pathophysiological mechanisms and clinical implications. *Acta Neurochir* 1998;71(Suppl):282–284.
  34. Allt G, Lawrenson JG. Is the pial microvessel a good model for response in blood-brain barrier studies? *Brain Res Brain Res Rev* 1997;24:67–76.
  35. Revest PA, Jones HC, Abbott NJ. Transendothelial electrical potential across pial vessels in anaesthetised rats: A study of ion transport at the blood-brain barrier. *Brain Res* 1994;652:76–82.